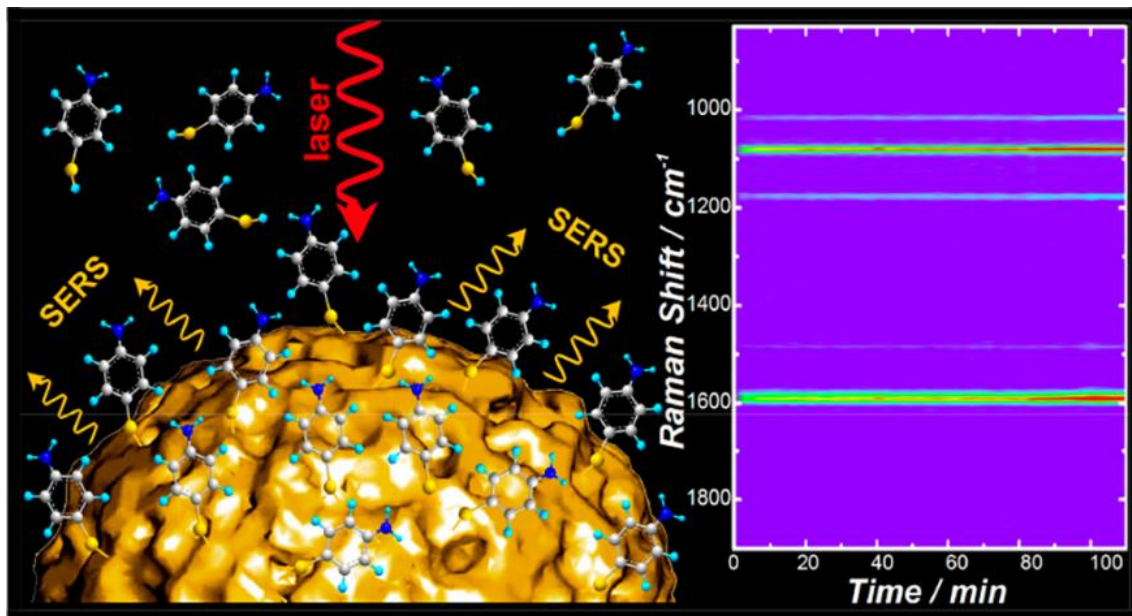


Nanoscale Surface Curvature Effects on Ligand–Nanoparticle Interactions: A Plasmon–Enhanced Spectroscopic Study of Thiolated Ligand Adsorption, Desorption, and Exchange on Gold Nanoparticles

Esteban Villarreal, Guangfang Grace Li, Qingfeng Zhang, Xiaoji Fu, and Hui

Wang
 Department of Chemistry and Biochemistry, University of South Carolina, Columbia, South Carolina 29208, United States

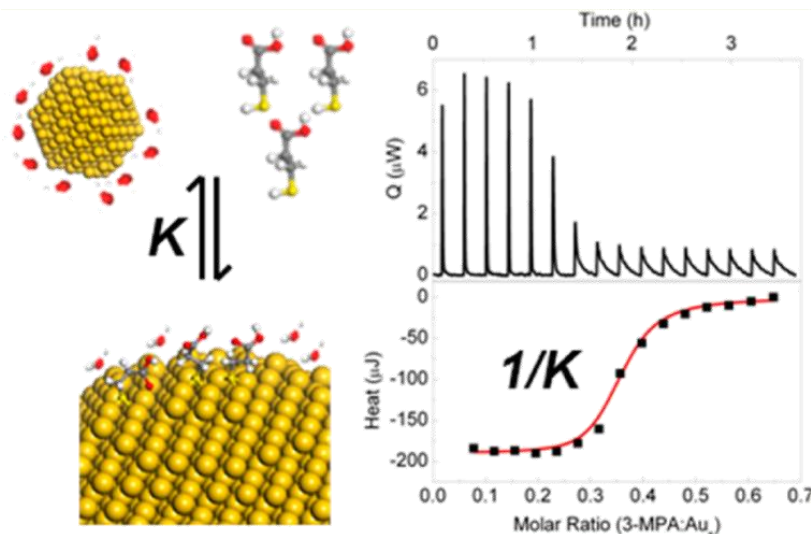


DOI: 10.1021/acs.nanolett.7b01593
 Nano Lett. 2017, 17, 4443–4452

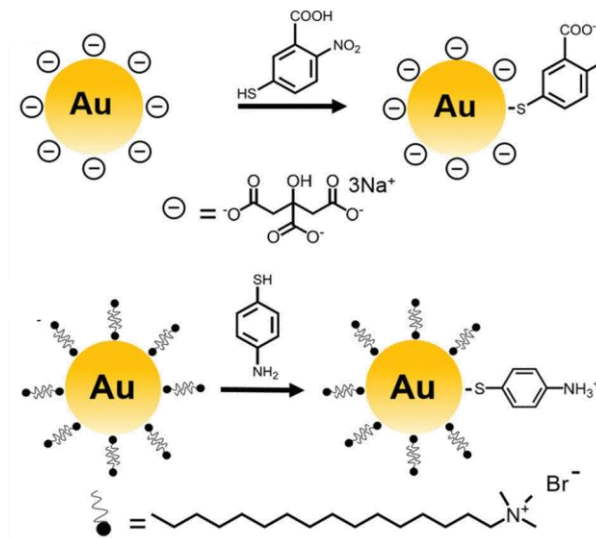
Tripti Ahuja
 27/10/18

Introduction (Why this paper?)

- Organic capping ligands play a pivotal role in guiding nanocrystal growth during bottom-up synthesis.
- Functionalization of these nanocrystals with desired ligands through ligand-guided crystal growth or post-ligand exchange reaction introduce interesting modifications to optical, electronic and surface properties of the nanoparticles which influences a series of important interfacial processes like surface charge transfer, catalytic molecular transformations, targeted drug delivery, and even to form self-assembled suprastructures.
- Detailed mechanistic understanding of ligand interactions with nanoparticle core is crucial.
- Energetics and dynamics of ligand surface interactions are drastically modified when nanoscale curvatures are introduced to the planar surfaces.
- A series of in-situ spectroscopic studies have been used to study these curvatures effect to resolve the complex kinetic and thermodynamic profiles of nanoparticles–ligand interactions



Thermodynamic Profiles at the Solvated Inorganic-Organic Interface: The Case of Gold-Thiolate Monolayers
 Nano Lett. 2013, 13, 4442–4448



Measuring binding kinetics of aromatic thiolated molecules with nanoparticles via surface-enhanced Raman spectroscopy, *Nanoscale*, 2015, 7, 8766

ACCOUNTS
 of chemical research

**The Chemistry of the Sulfur–Gold Interface:
 In Search of a Unified Model**
 2012, 8, 1183–1192

In this paper...

- They have scrutinize how the nanoscale surface curvature profoundly impacts the binding affinity and cooperativity as well as the adsorption/ desorption/ exchange kinetics of thiolated aromatic ligands on surface-textured AuNPs using surface enhanced Raman scattering (SERS) as an ultrasensitive plasmon -enhanced spectroscopic tool.
- Using SERS, they study real time direct correlation of ligand dynamics with interfacial molecular structures, both at equilibrium and non-equilibrium conditions without separating the colloidal NPs from their native, ligand-present environments.
- They have synthesized subwavelength (~130 nm) Au quasi-spherical nanoparticles (QSNPs) and surface-roughened nanoparticles (SRNPs) by kinetically maneuvering the seed-mediated nanocrystal growth.
- They used these subwavelength NPs to circumvent the irreproducibility issues of hotspots. SERS based quantification and characterization of surface ligands on NPs surfaces were performed.
- Effect of flat facets versus curved facets of similar size NPs on ligand dynamics was studied.

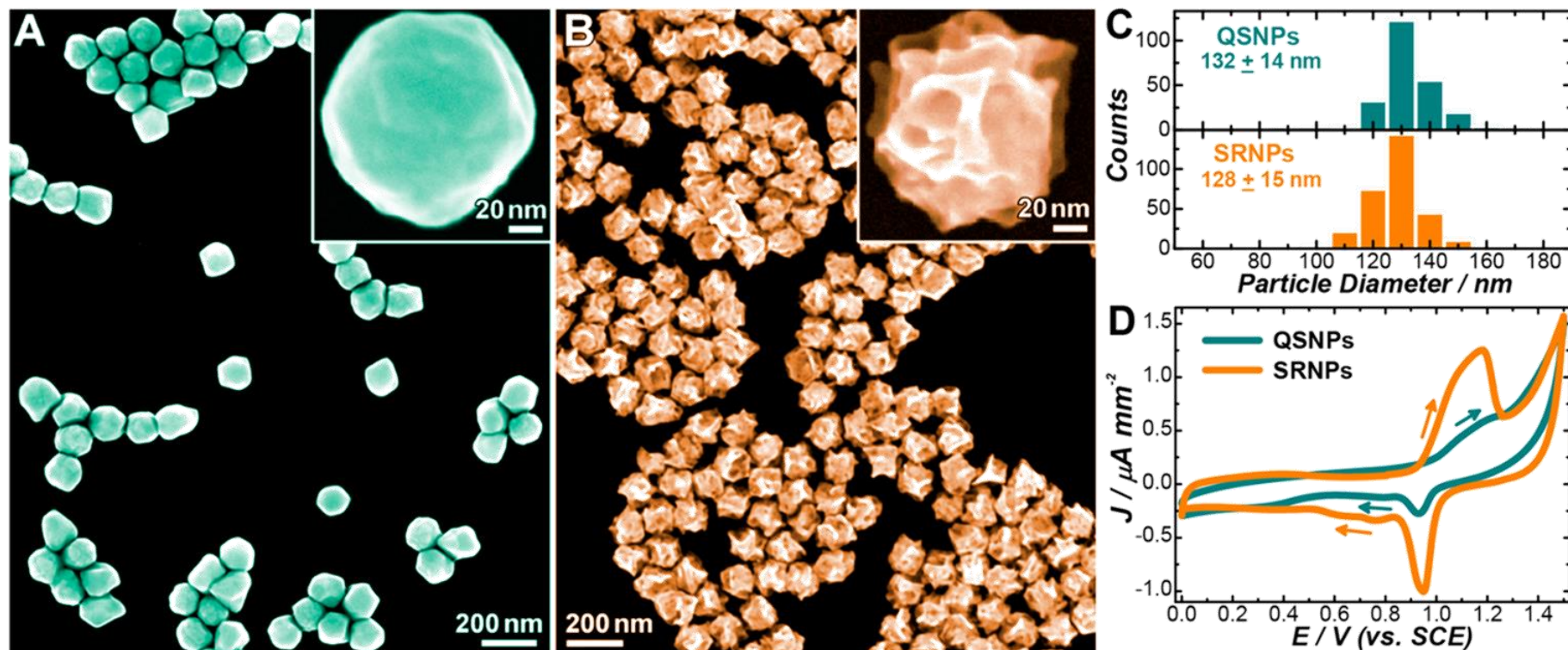


Figure 1. Structures of Au QSNPs and SRNPs. SEM images of Au (A) QSNPs and (B) SRNPs. The insets show higher-magnification SEM images highlighting the nanoscale surface textures of individual particles. (C) Size distributions of Au QSNPs and SRNPs. The average particle sizes and standard deviations were obtained from more than 200 nanoparticles in SEM images. (D) CV curves of Au QSNPs and SRNPs in 0.5 M H₂SO₄ electrolyte at a potential sweep rate of 5 mV s⁻¹. The arrows show the directions of the potential sweeps.

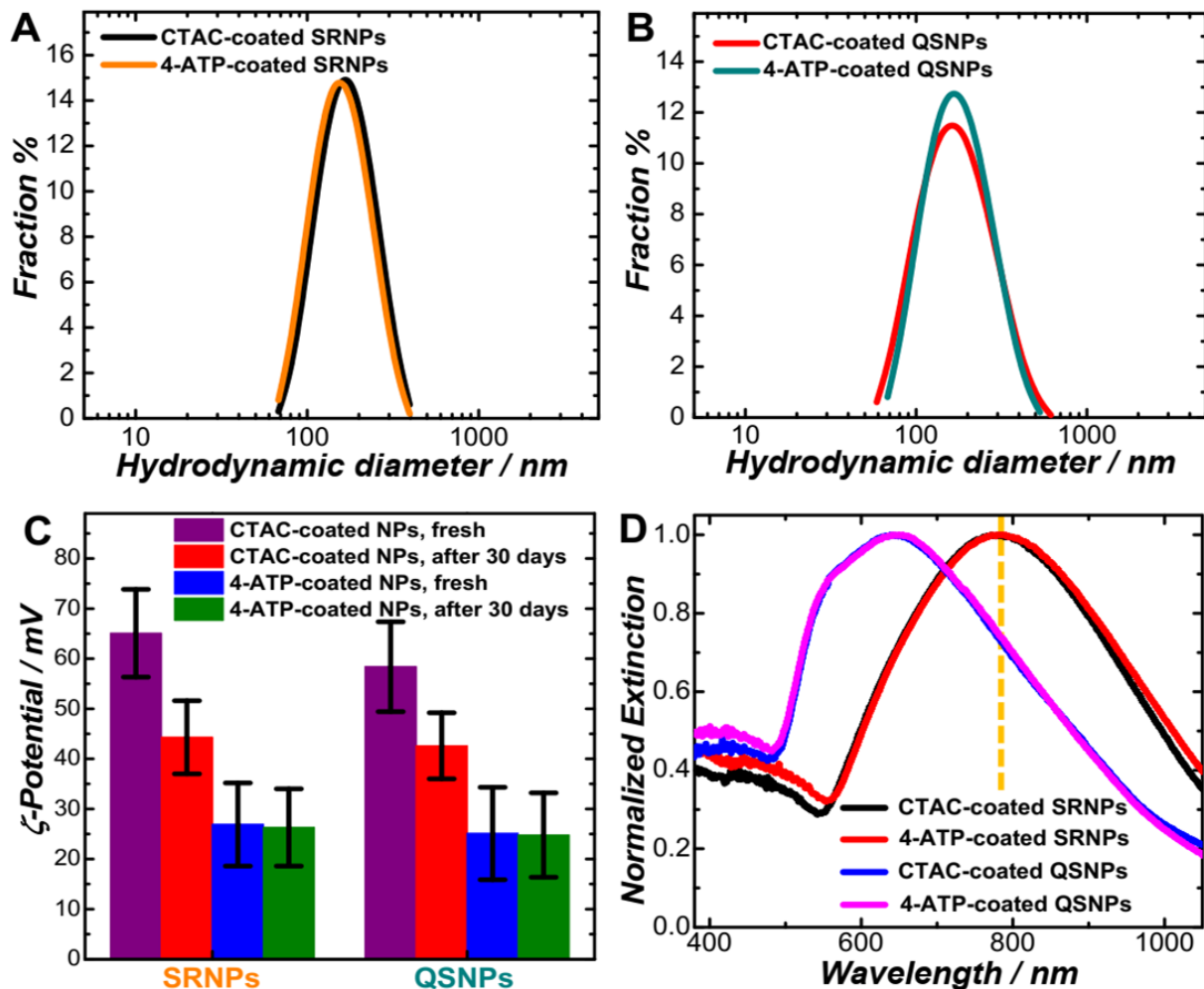


Figure S1. Hydrodynamic diameters of (A) Au SRNPs and (B) Au QSNPs before 4-ATP adsorption and after incubation with 50 μ M of 4-ATP for 24 h. (C) ζ -potentials of freshly prepared CTAC-coated and 4-ATP-coated NPs and the NPs after being store in water for 30 days at room temperature. (D) Extinction spectra of colloidal CTAC-coated and 4-ATP-coated Au SRNPs and Au QSNPs. The vertical dash line shows the wavelength (785 nm) of the excitation laser for SERS measurements.

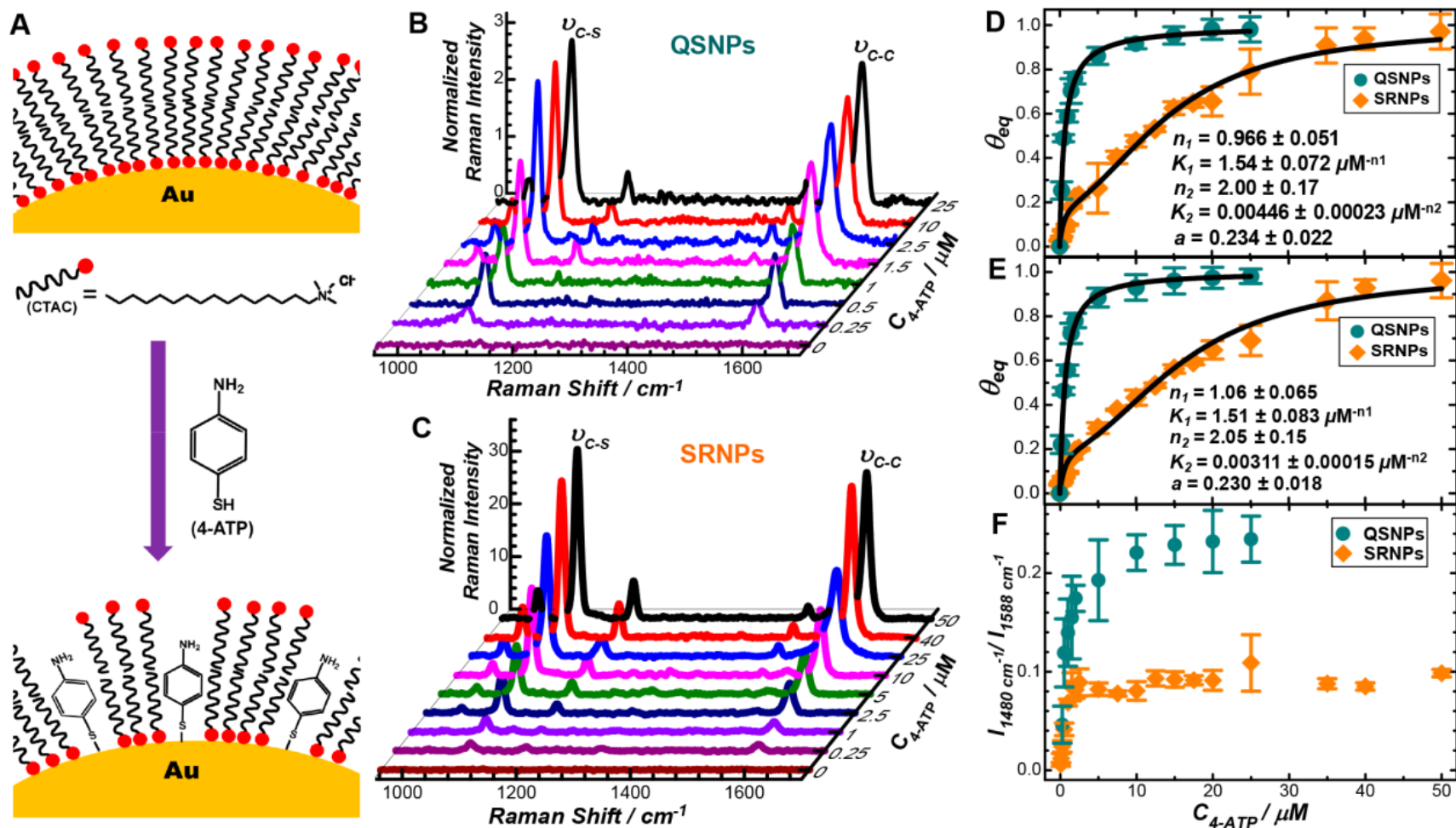


Figure 2. Thermodynamics of 4-ATP adsorption on Au QSNPs and SRNPs. (A) Schematic illustration of ligand displacement of CTAC with 4-ATP. SERS spectra collected on (B) QSNPs and (C) SRNPs after the nanoparticles were incubated with various concentrations of 4-ATP for 24 h. The peak intensity at 3230 cm^{-1} (normal Raman peak of H₂O) was used as the internal reference for signal normalization. The 4-ATP adsorption isotherms on Au QSNPs and SRNPs obtained from the (D) 1078 cm^{-1} and (E) 1588 cm^{-1} modes. The solid black curves show the least-squares curve fitting results. (F) Plots of $I_{1480 \text{ cm}^{-1}} / I_{1588 \text{ cm}^{-1}}$ versus $C_{4\text{-ATP}}$ for Au QSNPs and SRNPs. The error bars represent the standard deviations obtained from five replicate samples.

Equations used:

$$\theta_{\text{eq}} = \frac{K_1 C^{n_1}}{1 + K_1 C^{n_1}} \quad (\text{i}) \quad \theta_{\text{eq}} = a \times \frac{K_1 C^{n_1}}{1 + K_1 C^{n_1}} + (1 - a) \times \frac{K_2 C^{n_2}}{1 + K_2 C^{n_2}} \quad (\text{ii})$$

Classical Langmuir adsorption isotherm

Non -classical Langmuir adsorption isotherm
or two component Hill equation

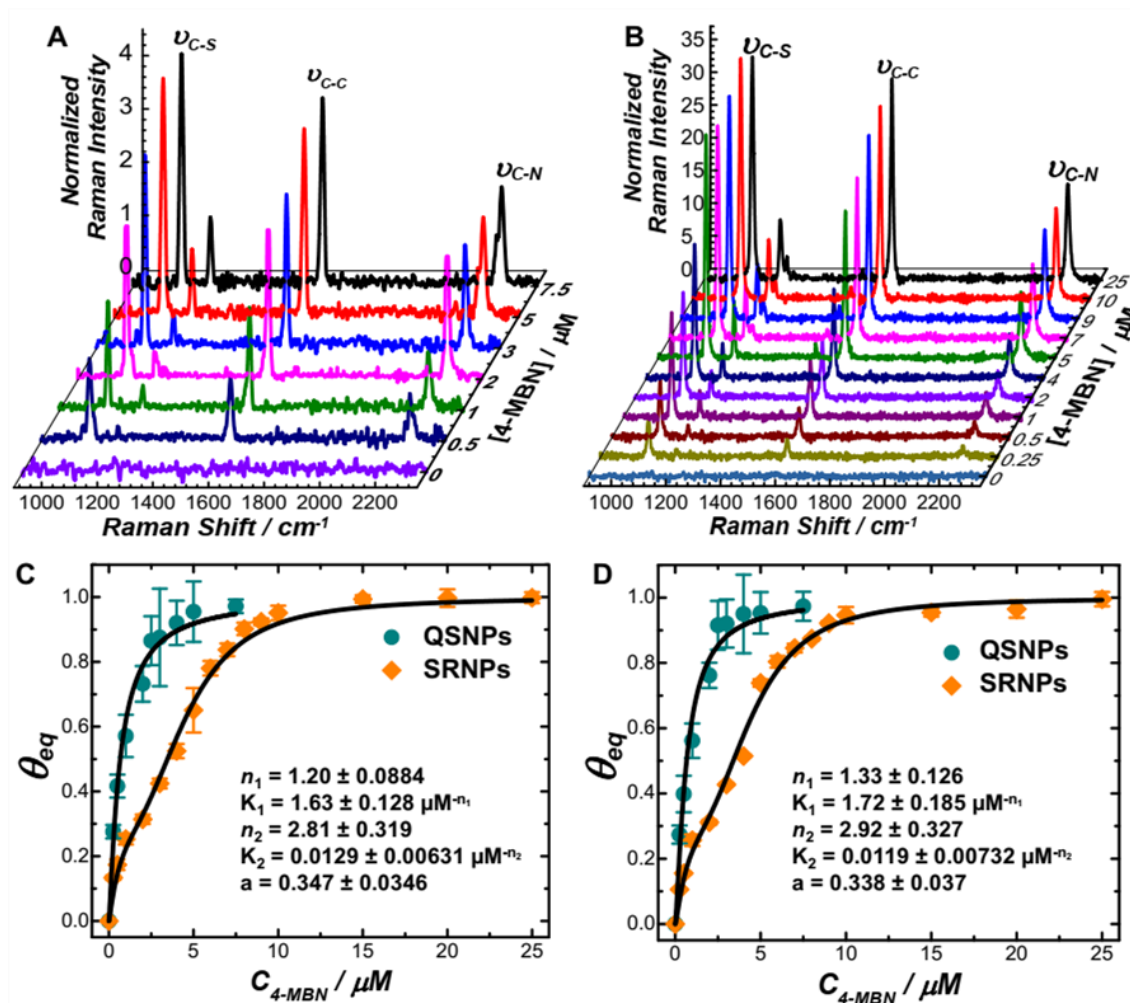
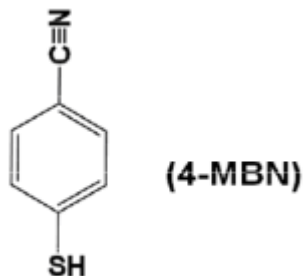


Figure S5. SERS spectra collected on colloidal (A) Au QSNPs and (B) Au SRNPs after the nanoparticles were incubated with various concentrations of 4-MBN for 24 h. The peak intensity at 3230 cm^{-1} (normal Raman peak corresponding to the O-H stretching mode of H₂O) was used as the internal reference for signal normalization. 4-MBN adsorption isotherms (plots of apparent surface-coverage of 4-MBN $\theta_{4\text{-MBN}}$ vs concentration of 4-MBN $C_{4\text{-MBN}}$) on the surfaces of Au QSNPs and SRNPs obtained from the (C) 2226 cm^{-1} mode and (D) 1588 cm^{-1} mode in the SERS spectra. The error bars represent the standard deviations obtained from 5 replicate samples prepared under identical conditions. The solid black curves show the least squares curve fitting results. The R² values were all greater than 0.98.

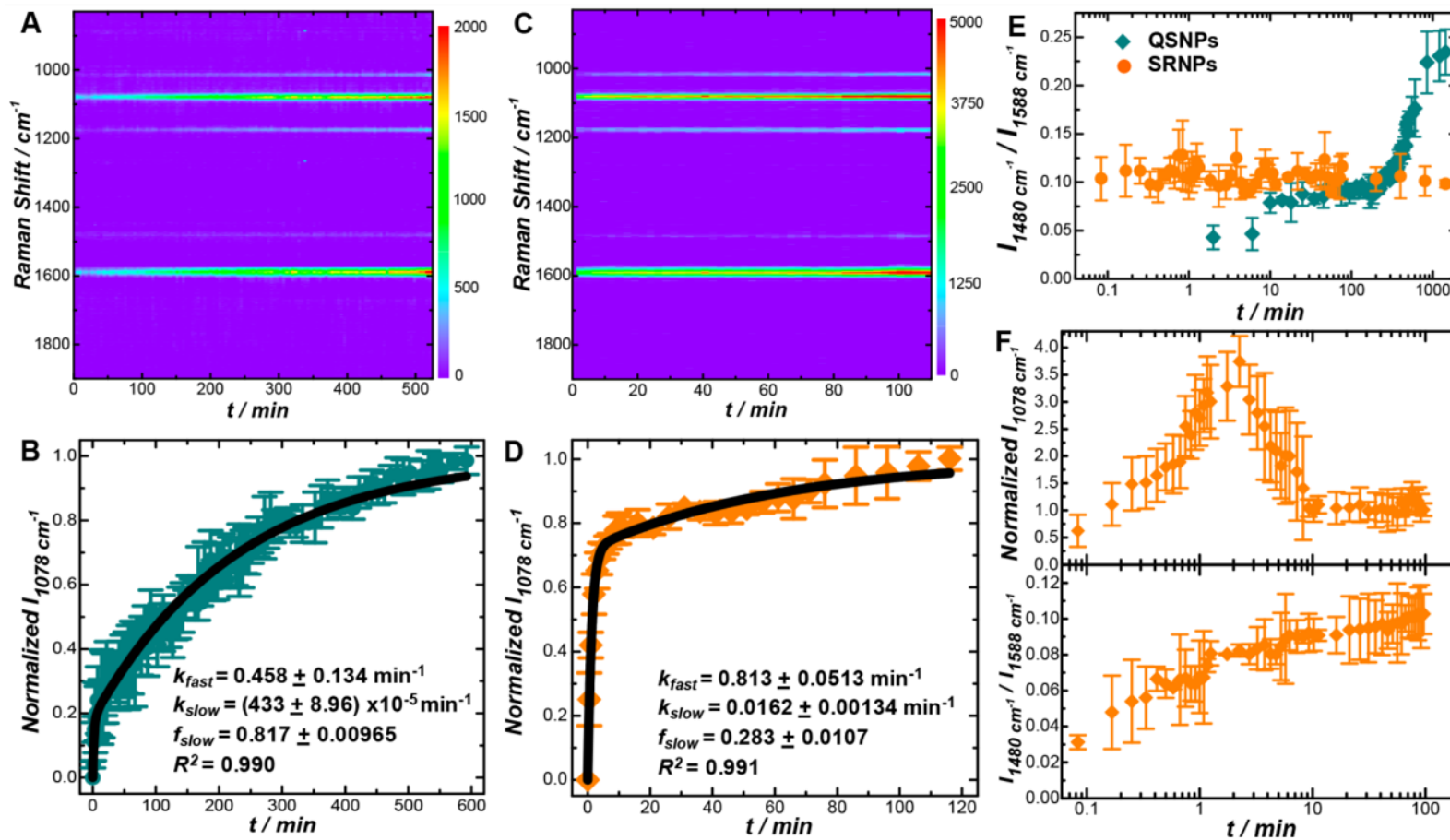


Figure 3. Kinetics of 4-ATP adsorption on Au QSNPs and SRNPs. Time-resolved SERS spectra of colloidal (A) QSNPs and (C) SRNPs incubated with 50 μM 4-ATP at room temperature. Temporal evolution of SERS intensities of the 1078 cm^{-1} mode upon exposure of (B) QSNPs and (D) SRNPs to 50 μM 4-ATP. The SERS intensities of the 1078 cm^{-1} mode were normalized against the values obtained after the adsorption/desorption equilibrium was reached (24 h incubation). The solid black curves show the least-squares curve fitting results. (E) Temporal evolution of $I_{1480 \text{ cm}^{-1}}/I_{1588 \text{ cm}^{-1}}$ during incubation of Au SRNPs and QSNPs with 50 μM 4-ATP. (F) Temporal evolution of the intensity of the 1078 cm^{-1} mode (upper panel) and $I_{1480 \text{ cm}^{-1}}/I_{1588 \text{ cm}^{-1}}$ (lower panel) upon exposure of SRNPs to 2.0 μM 4-ATP. The error bars represent the standard deviations obtained from five independent experimental runs.

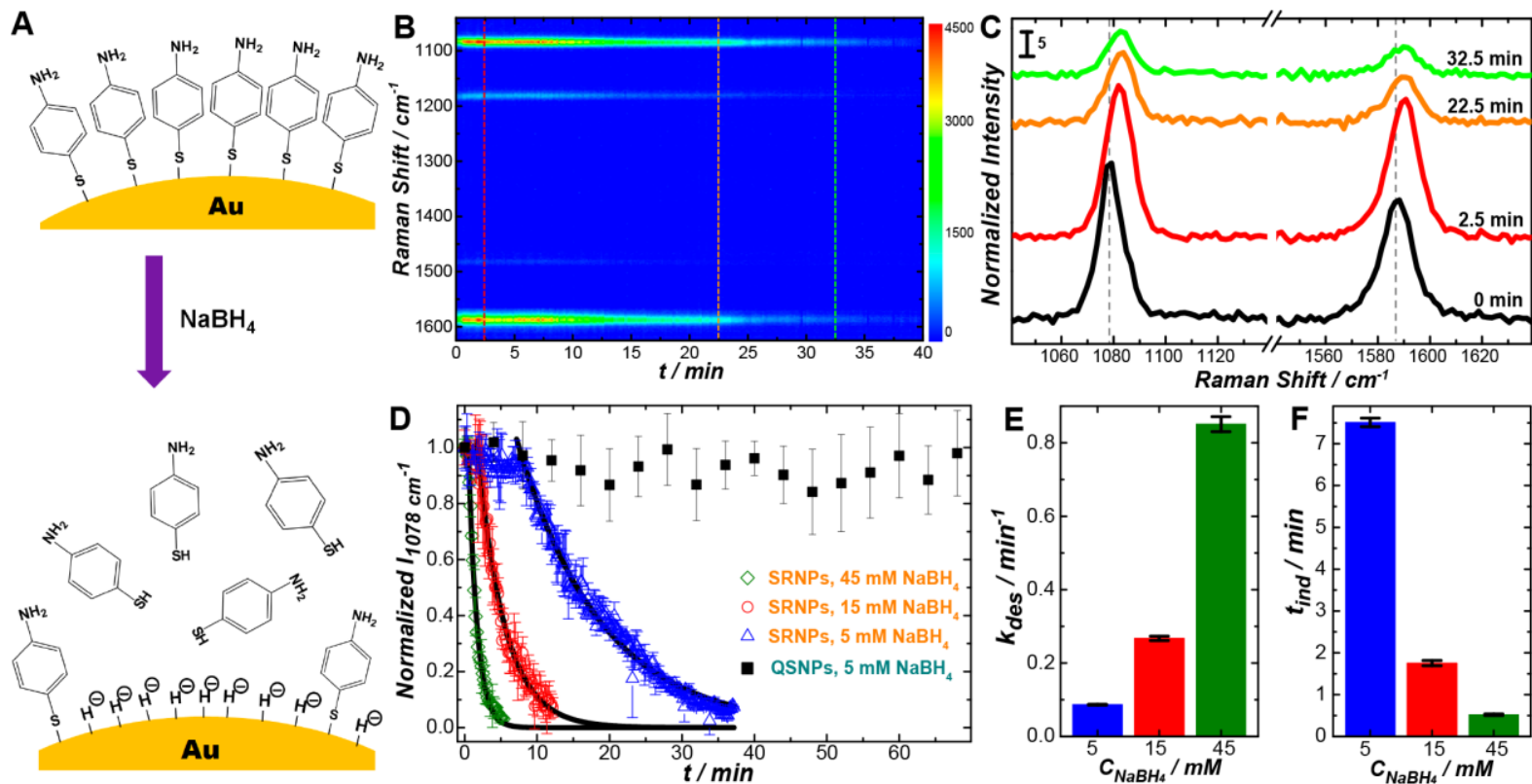


Figure 4. NaBH_4 -induced desorption of 4-ATP ligands. (A) Schematic illustration of NaBH_4 -induced desorption of 4-ATP from Au nanoparticle surfaces. (B) Time-resolved SERS spectra of 4-ATP-coated SRNPs upon exposure to 5 mM NaBH_4 at room temperature. (C) Representative snapshot SERS spectra collected at 0, 2.5, 22.5, and 32.5 min. The Raman signals were normalized using the O-H stretching mode of H_2O as the internal reference. The spectra were offset for clarity. (D) Temporal evolution of SERS intensities at 1078 cm^{-1} for 4-ATP-coated SRNPs and QSNPs exposed to various concentrations of NaBH_4 . The SERS intensities were normalized against the initial peak intensities of the 1078 cm^{-1} mode. The error bars represent the standard deviations obtained from five independent experimental runs. The solid black curves show the least-squares curve fitting results. (E) k_{des} and (F) t_{ind} for the 4-ATP desorption from Au SRNPs at various C_{NaBH_4} .

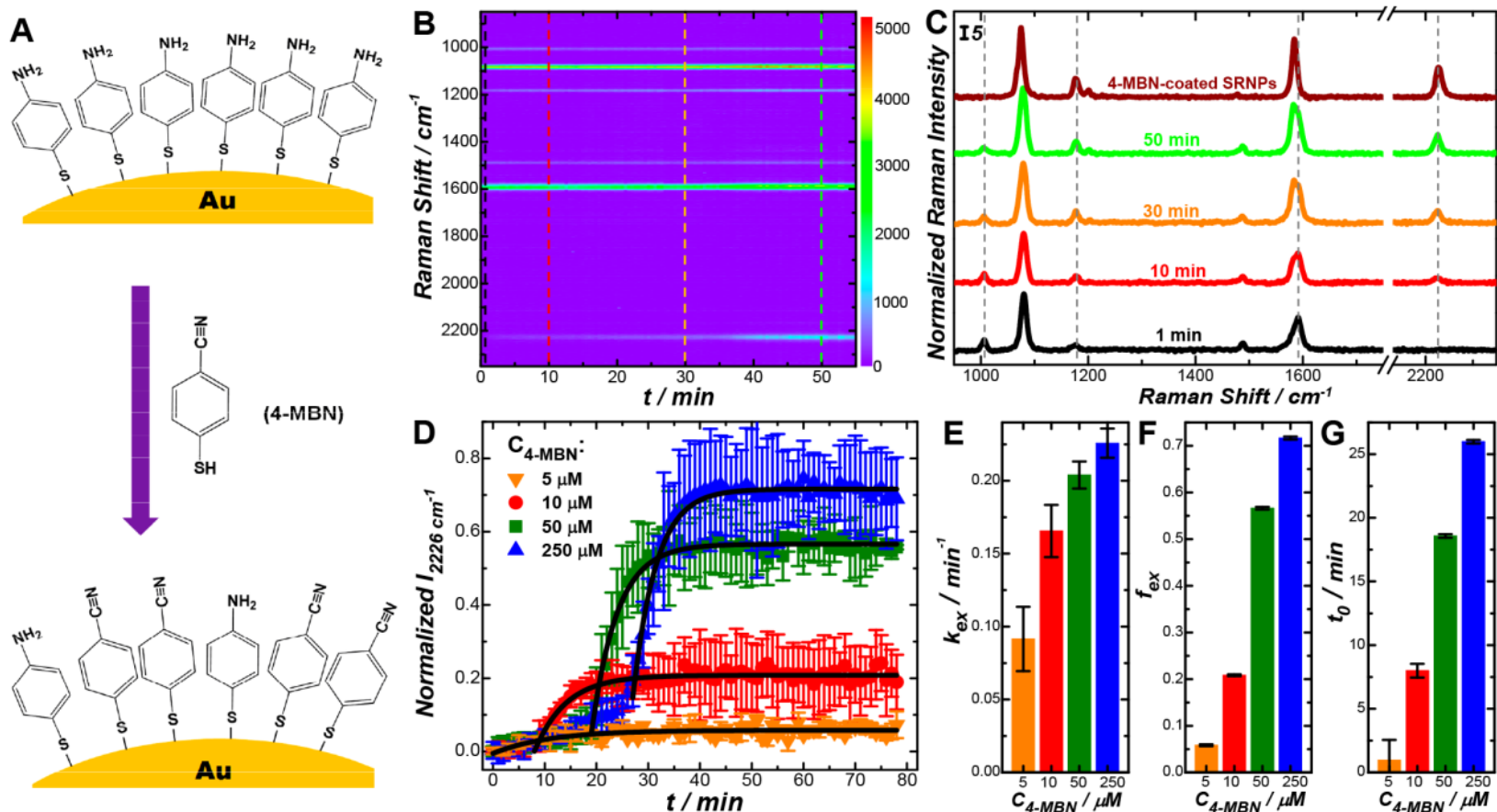


Figure 5. Thiolated ligand exchange on highly curved nanoparticle surfaces. (A) Schematic illustration of ligand exchange of 4-ATP with 4-MBN on Au nanoparticle surfaces. (B) Time-resolved SERS spectra of 4-ATP-coated SRNPs (obtained through incubation of CTAC-coated SRNPs with 100 μM 4-ATP for 24 h) after exposure to 250 μM 4-MBN at room temperature. (C) Representative snapshot SERS spectra collected at 1, 10, 30, and 50 min. The SERS spectra of SRNPs fully covered with 4-MBN (obtained after incubating the CTAC-coated SRNPs with 100 μM 4-MBN for 24 h) was also shown for comparison. The Raman signals were normalized using the O-H stretching mode of H₂O as the internal reference. The spectra were offset for clarity. (D) Temporal evolution of SERS intensities of the 2226 cm⁻¹ mode upon exposure of 4-ATP-coated Au SRNPs to various concentrations of 4-MBN. The peak intensities were normalized against the intensity of the 2226 cm⁻¹ peak of the SRNPs with saturated 4-MBN coverages. The error bars represent the standard deviations obtained from five independent experimental runs. The solid black curves show the least squares curve fitting results. (E) k_{ex}, (F) f_{ex}, and (G) t₀ at various C_{4-MBN}.

Conclusions

- ✓ This work gave insights on the complicated thermodynamic and kinetic landscapes underlying the surface curvature dependent adsorption, desorption and exchange behavior of thiolated ligands on AuNPs surfaces.
- ✓ It guides us to fine-tailor the surface chemistry on NPs for specific applications like targeted drug delivery, multi-modality bioimaging, sensing and photonics.
- ✓ The surface curvature dependent interfacial ligand behaviors forms the keystone for the site-selective functionalization of NPs surfaces, allowing different chemical reactions and intermolecular interactions to occur at different sites of the same NPs.
- ✓ These SERS based studies distinguished the ligand dynamics on highly curved surfaces versus atomically flat facets of AuNPs efficiently.

Author's future perspectives

- ✓ How much atomic-level surface curvature (such as each high index facet of curved surfaces of SRNPs) on the subnanometer length scale affects the interfacial ligand behaviors is still elusive.
- ✓ Nature of different types (positive, negative and neutral) of curvatures of SRNPS need to be studied.
- ✓ Understanding the nanoparticle surface chemistry towards high level of comprehensiveness and depth.